

Nanoscale wire formation on sputter-eroded surfaces

J. Kim^{a)} and B. Kahng

School of Physics and Center for Theoretical Physics, Seoul National University, Seoul 151-747, Korea

A.-L. Barabási

Department of Physics, University of Notre Dame, Notre Dame, Indiana 46556

(Received 16 January 2002; accepted 17 September 2002)

Rotated ripple structures (RRS) on sputter-eroded surfaces are potential candidates for nanoscale wire fabrication. We show that the RRS can form when the width of the collision cascade in the longitudinal direction is larger than that in the transverse direction and the incident angle of ion beam is chosen in a specific window. By calculating the structure factor for the RRS, we find that they are more regular and their amplitude is more enhanced compared to the much studied ripple structure forming in the linear regime of sputter erosion. © 2002 American Institute of Physics. [DOI: 10.1063/1.1519963]

The fabrication of nanoscale surface structures such as quantum dots and quantum wires, have attracted considerable attention due to their applications in optical and electronic devices.¹ Yet, the nanostructures obtained in various self-assembled ways have a size distribution wider than required by applications, and display random alignment. Lithographic methods² are often considered prime candidates to overcome these shortcomings, but their limited resolution offers further challenges. Consequently, there is continued high demand for alternative methods that would allow low cost and efficient mass fabrication of nanoscale surface structures. In the light of these technological and scientific driving forces, the recent demonstration by Facsko *et al.* that low-energy (40 eV~1.8 keV) normal incident Ar⁺ sputtering on GaSb (100) surfaces leads to nanoscale islands which display remarkably good hexagonal ordering and have a uniform size distribution, has captured the interest of the scientific community.^{3,4}

It is known that the morphological evolution of a sputter-eroded surface is well approximated by the noisy nonlinear Kuramoto–Sivashinsky (KS) equation,

$$\begin{aligned} \partial_t h = \nu_x \partial_x^2 h + \nu_y \partial_y^2 h - D_{xx} \partial_x^4 h - D_{yy} \partial_y^4 h - D_{xy} \partial_x^2 \partial_y^2 h \\ + \frac{\lambda_x}{2} (\partial_x h)^2 + \frac{\lambda_y}{2} (\partial_y h)^2 + \xi(x, y, t), \end{aligned} \quad (1)$$

where ν_x and ν_y are the effective surface tensions generated by the erosion process; D_{xx} , D_{yy} , and D_{xy} are the ion induced effective diffusion constants; λ_x and λ_y describe the tilt-dependent erosion rates in each direction; and $\xi(x, y, t)$ is an uncorrelated white noise with zero mean, mimicking the randomness resulting from the stochastic nature of ion arrival to the surface.^{5,6} At low temperatures all the coefficients in Eq. (1) depend on experimental parameters such as the ion beam flux f , the ion beam energy ϵ , and the incidence angle of ion beam θ ,⁷ while at high temperatures D is the relaxation rate due to surface diffusion, depending on surface

temperature.⁸ For the sputter erosion process $\nu < 0$ and $D > 0$, while the signs of λ_x and λ_y vary depending on the incident angle of the ion beam.^{5,6}

Recently numerical simulations have shown that there is a clear separation of the linear and nonlinear regimes in time:⁹ Up to a crossover time τ_1 the surface is eroded as if the nonlinear terms would be completely absent, following the predictions of the linear theory⁸ [i.e. $\lambda_x = \lambda_y = 0$ in Eq. (1)]. After τ_1 , however, the nonlinear terms with coefficients λ_x and λ_y take over and completely determine the surface morphology.

In the nonlinear regime the case $\lambda_x \lambda_y < 0$ is in particular interesting. The surface morphology in this case exhibits another transition from kinetic roughening to a rotated ripple structures (RRS) at a second crossover time τ_2 ($\tau_2 > \tau_1$), as first predicted by Rost and Krug,¹⁰ and observed numerically in Ref. 9. While the presence of the RRS was proposed theoretically, the structure has not been observed experimentally yet. In this letter we investigate the necessary conditions for the formation of RRSs and the impact of the various experimentally controllable parameters on the morphology of the RRS. We find that at low temperatures the RRSs can form when the longitudinal width (σ) of the damage cascade generated by the ion beam is larger than the transverse width (μ) and the angle of the incident beam is chosen in a rather narrow window.

The RRSs orient with the angle given by $\phi_c = \tan^{-1} \sqrt{-\lambda_x / \lambda_y}$,¹⁰ at which one of the nonlinear term in the rotated frame (x', y'), say $\lambda'_{x'}$, vanishes. We find that the angle ϕ_c increases with the ratio $a_\mu = a / \mu$, but decreases with the incident angle θ (Fig. 1), where a denotes the penetration depth of the ion beam. Since a_μ depends on ϵ and θ , which are adjustable, the orientation of the RRS is experimentally controllable. The KS equation in the rotated frame can be written in a similar form to Eq. (1) but the two that first, the coefficients ν , D , and λ , are replaced by ν' , D' , and λ' , which are functions of those in the original frame and the angle ϕ_c , and second, the cross terms, $\nu'_{x'y'} \partial_{x'} \partial_{y'} h$, $D'_{x'y'} \partial_{x'}^2 \partial_{y'}^2 h$, and $\lambda'_{x'y'} (\partial_{x'} h) (\partial_{y'} h)$, are present.

In the rotated frame since $\lambda'_{x'}$ vanishes, the dynamic

^{a)}Present address: Supercomputing Research Department, KISTI, Daejeon 305-806, Korea.

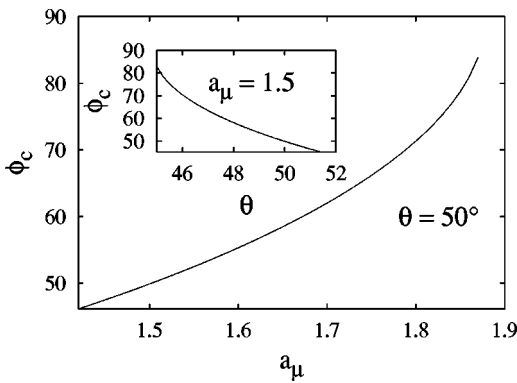


FIG. 1. The rotation angle ϕ_c as a function of a_μ at $\theta=50^\circ$. The inset shows ϕ_c vs θ for $a_\mu=1.5$. The rotation angle increases as the ratio a_μ increases, but decreases with the incident angle θ .

equation in the x' direction becomes effectively linear, because the effects by the two cross terms, $\nu'_{x'y'}\partial_{x'}\partial_{y'}h$, and $D'_{x'y'}\partial_{x'}^2\partial_{y'}^2h$ are negligible. Consequently, the ripple pattern is along the x' direction as long as (i) $\nu'_{x'}<0$; (ii) $D'_{x'x'}>0$; and (iii) $\lambda_x\lambda_y<0$. Therefore conditions (i), (ii), and (iii) are the necessary conditions for the formation of the RRS.

We investigate the satisfiability of these conditions in the parameter space $(\theta, a_\mu = a/\mu)$ for different values of $a_\sigma = a/\sigma$. We find that when $a_\mu > 1$ and $a_\sigma = 1$ or $a_\mu > 2$ and $a_\sigma = 2$, the RRS can form in the region depicted in Fig. 2. For $a_\mu < 1$ given $a_\sigma = 1$, the shaded region satisfying (i)–(iii) scarcely exists, so that the formation of RRS is less likely. That means the RRSs are expected to form when the longitudinal width σ is larger than the transverse width μ , that is, $\sigma > \mu$. It is not known explicitly how the two characteristic widths σ and μ depend on experimental parameters. However, based on the recent experimental result that for graphite surfaces σ depends on ϵ , while μ is independent of ϵ for large ϵ ($2 \sim 50$ keV),¹¹ we would say that the $\sigma > \mu$ condition could be met when the energy of the incident ion beam is high enough. The use of a high energy ion beam however increases τ_2 rapidly, requiring a longer exposure time. Besides the condition $\sigma > \mu$, we have to choose the incident angle appropriately (Fig. 2). The window of such angles is rather narrow.

Since the nonlinear term disappears in the x' direction the surface in this direction is driven by a linear instability. The amplitude of the RRS grows exponentially with time until the nonlinear term in the y' direction becomes effective,

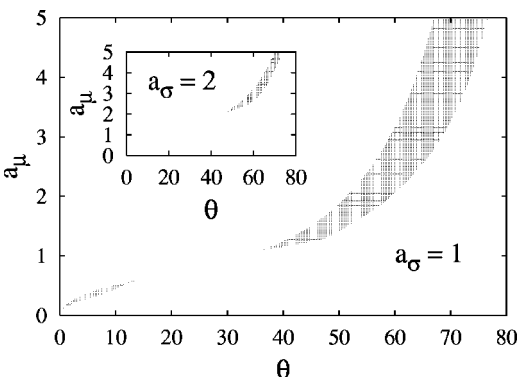


FIG. 2. The shaded region in the parameter space (θ, a_μ) for $a_\sigma=1$ (inset: for $a_\sigma=2$) corresponds to the region where the RRS can form.

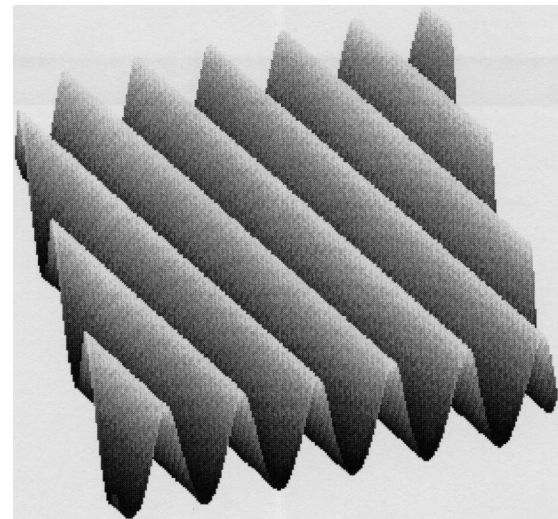


FIG. 3. Surface morphology of the RRS, as generated by numerical simulations, with $a_\mu=1.3$, $a_\sigma=1$ and $\theta=43.56^\circ$.

after which the amplitude saturates due to the cross term, $\lambda'_{x'y'}(\partial_{x'}h)(\partial_{y'}h)$. Meanwhile, since the surface in the y' direction displays kinetic roughening, the roughness in the y' direction is considerably reduced compared with the roughness in the x' direction. Therefore, the RRS develops a rough morphology in the x' direction, while it is relatively smooth in the y' direction, the end configuration resembling a V-shaped wire pattern, as shown in Fig. 3.¹² The RRS formed in the nonlinear regime is comparable with the ripple pattern formed in the linear regime, where there are modulations in both directions, and the roughness in each direction is almost of the same order.

We also examined the structure factor, which is the Fourier transform of the height–height correlation function, averaged over different configurations.¹³ We find that the structure factor exhibits a peak at $(q_{x,c}, q_{y,c})$, corresponding to $(q'_{x',c}, 0)$ in the rotated coordinates (Fig. 4). The $q'_{y',c} = 0$ fact results from that there is no characteristic length scale along the y' direction, implying that the RRS is straight along the y' direction. The peak of the structure factor for

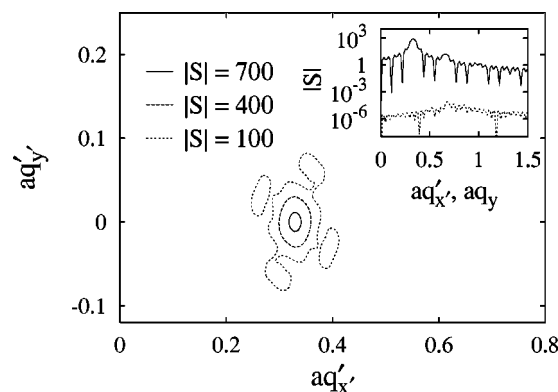


FIG. 4. The amplitude of the structure factor $|S(\mathbf{q}')|$ for the RRS shown in Fig. 3. The peak of the structure factor is at $aq'_{x,c}=0.33$ and $q'_{y,c}=0$, implying that the wire structure is straight along the y' axis. The inset shows the comparison between the amplitudes of the structure factor for the RRS (solid line) and for the linear ripple (dotted line), implying the amplitude of the RRS is about a factor of 10^7 larger compared to that of the ripple structure formed in the linear regime.

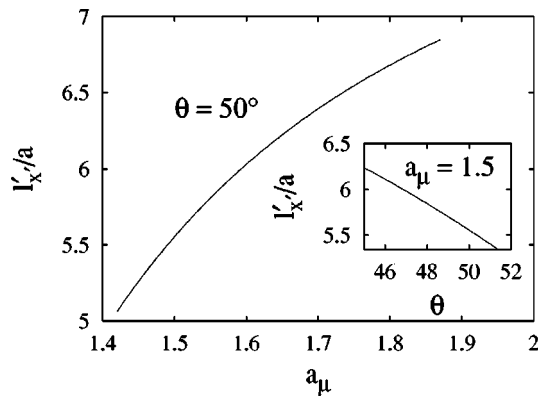


FIG. 5. The wavelength of the RRS in units of a as a, showing function of a_μ ($\theta=50^\circ$). Inset: The wavelength vs θ at $a_\mu=1.5$.

the RRS is much sharper than that for the ripple structure formed in the linear regime in the comparison shown in the inset of Fig. 4. Moreover, the amplitude of the structure factor for the RRS is much larger by the factor 10^7 compared to that for the ripple. Accordingly, the RRS could be a good candidate for the fabrication of nanowires.

Applying the linear instability theory in the x' direction we obtain the wavelength of the RRSs $\ell'_{x'} = 2\pi\sqrt{2D'_{x'x'}/|\nu'_{x'}|}$. The wavelength depends on the penetration depth linearly, i.e., $\ell'_{x'} \sim a$, independent of the ion flux f . In general, the penetration depth depends on the incident ion energy ϵ as $a \sim \epsilon^{2m}$, where $m \approx 1/4$ was obtained recently for the nanoscale dot structure in low energy sputtering.¹⁴ We also examined $\ell'_{x'}$ in function of the ratio a_μ and incident angle θ , observing a monotonically increasing and decreasing behavior, respectively (Fig. 5).

In the high temperature limit the wavelength of the RRS depends on the ion energy as $\ell'_{x'} \sim \epsilon^{-1/2}$, and on the ion flux as $\sim f^{-1/2}$, and on the temperature as $\sim \exp(-\epsilon/4k_B T)$, a dependence similar to that observed during the formation of nanoscale dots.¹⁵

In summary, we have examined the necessary conditions for the formation of RRSs, potential candidates for nanowires for electron transport. The RRS can be obtained when the longitudinal width σ of the damage cascade is larger than the transverse width μ with an appropriate selection of the angle of the incident ion beam. The angle window turns out to be rather narrow.

This work was supported by ONR, NSF-DMR 01-08494, NSF-INT 99-10426, and the Korean Research Foundation (Grant No. 99-041-D00150).

- ¹For a review, for example, see L. Jacak, P. Hawrylak, and A. Wojs, *Quantum Dots* (Springer, Berlin, 1998).
- ²T. I. Kamins and R. S. Williams, *Appl. Phys. Lett.* **71**, 1201 (1997).
- ³S. Facsko, T. Dekorsy, C. Koerdt, C. Trappe, H. Kurz, A. Vogt, and H. L. Hartnagel, *Science* **285**, 1551 (1999).
- ⁴F. Frost, A. Schindler, and F. Bigl, *Phys. Rev. Lett.* **85**, 4116 (2000).
- ⁵R. Cuerno and A.-L. Barabási, *Phys. Rev. Lett.* **74**, 4746 (1995).
- ⁶M. A. Makeev and A.-L. Barabási, *Appl. Phys. Lett.* **71**, 2800 (1997).
- ⁷M. Makeev, R. Cuerno, and A.-L. Barabási (unpublished).
- ⁸R. M. Bradley and J. M. E. Harper, *J. Vac. Sci. Technol. A* **6**, 2390 (1988).
- ⁹S. Park, B. Kahng, H. Jeong, and A.-L. Barabási, *Phys. Rev. Lett.* **83**, 3486 (1999).
- ¹⁰M. Rost and J. Krug, *Phys. Rev. Lett.* **75**, 3894 (1995).
- ¹¹S. Habenicht, W. Bolse, H. Feldermann, U. Geyer, H. Hofsass, K. P. Lieb, and F. Roccaforte, *Europhys. Lett.* **50**, 209 (2000).
- ¹²E. Kapon, D. Hwang, and R. Bhat, *Phys. Rev. Lett.* **63**, 430 (1989).
- ¹³S. K. Sinha, E. B. Sirota, S. Garoff, and H. B. Stanley, *Phys. Rev. B* **38**, 2297 (1988).
- ¹⁴S. Facsko, H. Kurz, and T. Dekorsy, *Phys. Rev. B* **63**, 165329 (2001).
- ¹⁵B. Kahng, H. Jeong, and A.-L. Barabási, *Appl. Phys. Lett.* **78**, 805 (2001).